

---

# A FACE RECOGNITION SYSTEM'S WORST MORPH NIGHTMARE, THEORETICALLY

---

Una M. Kelly, Raymond Veldhuis, Luuk Spreuwers

Faculty of EEMCS  
University of Twente  
Enschede

{u.m.kelly, r.n.j.veldhuis, l.j.spreuwers}@utwente.nl

## ABSTRACT

It has been shown that Face Recognition Systems (FRSs) are vulnerable to morphing attacks, but most research focusses on landmark-based morphs. A second method for generating morphs uses Generative Adversarial Networks, which results in convincingly real facial images that can be almost as challenging for FRSs as landmark-based attacks. We propose a method to create a third, different type of morph, that has the advantage of being easier to train. We introduce the theoretical concept of *worst-case morphs*, which are those morphs that are most challenging for a fixed FRS. For a set of images and corresponding embeddings in an FRS's latent space, we generate images that approximate these worst-case morphs using a mapping from embedding space back to image space. While the resulting images are not yet as challenging as other morphs, they can provide valuable information in future research on Morphing Attack Detection (MAD) methods and on weaknesses of FRSs. Methods for MAD need to be validated on more varied morph databases. Our proposed method contributes to achieving such variation.

**Keywords** Biometrics · Morphing Attack Detection · Face Recognition · Vulnerability of Biometric Systems

## 1 Introduction

Several publications have shown that Face Recognition Systems (FRSs) and humans are vulnerable to *morphing attacks*. A morph is an image that contains identity information from the faces of two different individuals. When such a morphed image is compared to an image of either contributing identity it is likely to be accepted as a match. This can lead to security risks in e.g. border control, since a criminal could travel using the identity document of an accomplice. Over the past few years, several methods to address such attacks have been proposed. In most cases, the morphs on which Morphing Attack Detection (MAD) methods are trained and tested are generated in-house, and are usually created by detecting corresponding landmarks in the faces, warping the images to an average geometry and then blending the pixel values (see Fig. 1) [1, 2, 3, 4].

The fact that MAD methods are often tested on datasets with similar characteristics as the sets used for training them may lead to overfitting to certain dataset-specific characteristics - especially if only one morphing algorithm was used [5, 6]. In many countries (e.g. the Netherlands) someone applying for an identity document can provide their own printed passport photo [7]. This means that before a passport photo is stored in an electronic Machine Readable Travel Document (eMRTD), it has been printed and scanned (P&S). During this process some morphing traces may be masked, which means an MAD method may perform differently on P&S morphs. Furthermore, the quality of automatically generated morphs is limited by the quality of the landmark detector used, while a criminal might spend more time to manually select landmarks. These are ways in which morphs can vary, even when the underlying algorithm with which they were generated is the same.

However, even if MAD methods are tested on datasets from different sources and that include P&S images, it is possible that there are other tools for generating morphs of which the research community is not yet aware. Therefore, it is necessary to explore other potential morphing tools in order to better understand the weaknesses of FRSs. Benchmarks

for validating MAD methods - such as [8, 9, 10] - can be extended and improved by evaluating morphs generated with different methods.

We introduce a new method for creating morphs in order to fill this gap. More precisely, we first examine which morphs are most challenging from the point of view of an FRS by exploiting the fact that FRSs are equipped with a (dis)similarity measure that is used to measure how similar two images are. Since this allows us to define the theoretically most challenging morph - the image that is most similar to two input images according to an FRS - we call these *worst-case morphs*. We then train a neural network to generate images that approximate these worst-case morphs. We examine how well our approximations of worst-case morphs can fool the FRS and whether this extends to other systems. Our results show that our morphs pose a significant threat to the FRS that was used to generate them, but that more work is needed to generate images that are truly close to worst-case morphs.

Our proposed system differs from GAN-based morphs [11, 12] that are also generated using a neural network. While GANs are trained to generate images from a low-dimensional embedding space (that is different from the embedding space of an FRS) that look as “real” as possible, we directly work with the embedding space of an FRS and its associated (dis)similarity measure to approximate the most challenging morph, without having the constraint that the image needs to look “real”. These two different goals could potentially be combined in future research.

Our main contributions are:

- a theoretical framework that when given a face recognition system and two images can be used to define a *worst-case morph*,
- showing how a deep-learning-based method can be applied to approximate worst-case morphs,
- examining how vulnerable two existing FRSs are to these morphs,
- providing a new method for generating morphs that leads to more variation in morph datasets and enables researchers to more accurately validate MAD methods in future work.

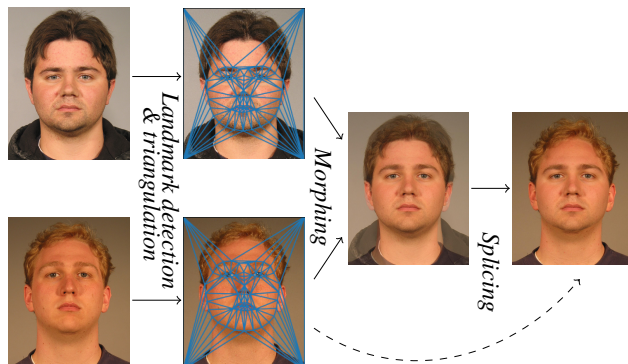


Figure 1: Landmark-based morphing process resulting in a *spliced* (sometimes called *complete*) morph.

## 2 Related Work

This section discusses variation in morphing algorithms in existing research. These morphs can be used to train and evaluate MAD methods, which can be either Single-Image MAD (S-MAD) methods - also called no-reference detection - or Differential MAD (D-MAD) methods.

[13] post-processes landmark-based morphs using a style transfer-based method in order to mask certain effects caused by the morphing process. [14] introduces a model to simulate the effects of P&S on images and [15] considers the influence of ageing on morphing attacks. However, if the underlying morphing algorithms use the same landmark-based method this provides limited information on the robustness of the detection method.

GANs were used in [12, 16] in an attempt to create a different type of morph, which was shown to be able to fool FRSs, if not as consistently as landmark-based morphs. By using existing generation networks from StyleGAN [17] and StyleGAN2 [17], and introducing Identity Priors, the results were improved in [11]. Since GANs are notoriously difficult to train [18] more stable methods for generating morphs would be useful.

[19] introduces an overview of S-MAD methods and discusses characteristics of the datasets used to train them. They address the lack of variation in morphing techniques by including morphs created using different algorithms as well as printed-and-scanned morphs in the evaluation of a multi-scale block binary pattern fusion approach for S-MAD. However, all morphing algorithms used are landmark-based and GAN morphs or other methods are not taken into consideration.

### 3 Proposed System

In this section we introduce a framework to generate images that approximate the worst-case morph, which is the image that is most similar to two input images according to the FRS.

Landmark-based morphing attempts to create images in image space that are similar to two given images. Instead, we use the embedding space of an FRS, since this should contain more structured information on the similarity of images. Let  $f$  be the function that describes an FRS’s mapping from the image space  $X$  to the embedding space  $Z$ :

$$\begin{aligned} f : X &\rightarrow Z \\ I &\mapsto z. \end{aligned}$$

Let  $d$  be a distance metric applied to  $Z$  by the FRS (i.e. it returns dissimilarity scores). In that case the *worst-case embedding* for two images  $I_1$  and  $I_2$  is

$$z^* := \operatorname{argmin}_{z \in Z} (\max [d(z, z_1), d(z, z_2)]), \quad (1)$$

where  $z_1 = f(I_1)$ ,  $z_2 = f(I_2)$ . For example, in the case that  $d(z_1, z_2)$  returns the euclidean distance between two embeddings  $z_1$  and  $z_2$ , the worst-case embedding becomes  $z^* = \frac{z_1 + z_2}{2}$ .

Equation 1 can be used for an FRS that returns dissimilarity scores. In the case of an FRS that uses similarity scores, defined by a function  $S$ , it becomes

$$z^* := \operatorname{argmax}_{z \in Z} (\min [S(z, z_1), S(z, z_2)]). \quad (2)$$

For example, if  $S(z_1, z_2)$  returns the cosine similarity, then  $S(z_1, z_2) = \cos(\theta)$ , where  $\theta$  is the angle between  $z_1$  and  $z_2$ . In that case  $z^*$  is any  $z$  for which  $S(z_1, z) = S(z, z_2) = \cos(\theta/2)$ .

A worst-case morph is an image  $M^*$  for which  $f(M^*) = z^*$ . We approximate  $M^*$  using a decoder  $D$  that maps from  $Z$  back to  $X$ , inverting the mapping of the FRS.  $D$  is trained to approximate a function  $f^{-1}$  that returns a preimage<sup>1</sup> of an embedding in  $Z$ :

$$\begin{aligned} f^{-1} : Z &\rightarrow X \\ z &\mapsto I' \in \{I | f(I) = z\}. \end{aligned}$$

If  $D$  can successfully reconstruct images, then our hypothesis is that  $D(z^*) = M \approx M^*$ . We call such morphs *embedding-based* morphs. While GAN-based morphs [11, 12] are also generated from embeddings using a decoder network, this is a different approach, since it does not directly use embeddings from the embedding space of an FRS.

#### 3.1 Morph generation

For our experiments, we rely on a ResNet34-based face recognition system. [20] We use the pretrained model `dlib_face_recognition_resnet_model_v1` from Dlib [21]. When given input images  $I_1$  and  $I_2$ , this FRS returns a 128-dimensional embedding for each image, resulting in  $z_1 = f(I_1)$  and  $z_2 = f(I_2)$ , where  $f$  describes the mapping defined by the neural network from the image space to the embedding space:

$$X = [0, 1]^{n_c \times w \times h} \quad \text{and} \quad Z = \mathbb{R}^{128},$$

where the number of colour channels  $n_c = 3$  and the image size  $w \times h = 224 \times 224$ . It can be used as a face verification system by calculating the euclidean distance between  $z_1$  and  $z_2$ .  $I_1$  and  $I_2$  are not accepted as a match if  $\|z_1 - z_2\|_2 > t$ , where  $t = 0.6$  is the recommended decision threshold. When using this threshold the system achieves an accuracy of 99.38% on LFW [21, 22].

In this case, the worst-case embedding  $z^*$  that minimises Eq. 1 is the embedding that lies on the interpolating line exactly between  $z_1$  and  $z_2$ . Thus a worst-case morph is any image  $M^*$  for which  $f(M^*) = \frac{z_1 + z_2}{2}$ . Note that, as mentioned in Section 3, using a different dissimilarity measure  $d$  would lead to a different  $z^*$  and  $M^*$ .

<sup>1</sup>It is highly unlikely that  $f$  is invertible.

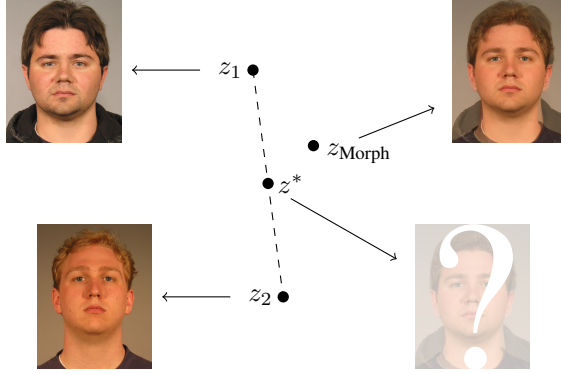


Figure 2: Visualisation of the difference between a landmark-based morph and the worst-case morph.

We train a network  $D$  with six deconvolutional layers to approximate  $f^{-1}$  by minimising

$$\mathcal{L}^i = \frac{1}{N} \sum_{(x,y) \in \text{pixels}} (I_{x,y}^i - D(f(I^i))_{x,y})^2, \quad (3)$$

where  $N$  is the number of pixels in the  $i$ -th image  $I^i$  in a mini-batch. The hyperparameters of this network can be found in the appendix. We train the network for 100 epochs. The loss function for one mini-batch with  $M$  images is

$$\mathcal{L} = \frac{1}{M} \sum_{i=1}^M \mathcal{L}^i. \quad (4)$$

When given two images  $I_1$  and  $I_2$  with corresponding embeddings  $z_1$  and  $z_2$ , we create an embedding-based morph by forwarding  $(z_1 + z_2)/2$  through the network.

## 4 Morph Evaluation

In this section we describe how to measure the vulnerability of two FRSs to landmark-based and embedding-based morphs. We examine the morphs with the same deep-learning-based FRS used for training the inverse network and a commercial system (Cognitec) [23], using the Mated Morph Presentation Match Rate (MMPMR( $t$ )), which is the proportion of (morphing) attacks for which both contributing identities are considered a match by the FRS when using a threshold  $t$  [24]. It is not always relevant whether an FRS considers *both* identities as a match, since for example during application for an eMRTD, the comparison of the applicant with the passport image may be performed by a human officer. For that reason we also share the scores of morphs compared with images of contributing identities in Section 6.

We set the threshold  $t$  to the recommended values for the respective FRSs and evaluate using a validation set. Dlib uses dissimilarity scores (distances) and has a recommended decision threshold of 0.6, the commercial system uses similarity scores and has a recommended decision threshold of 0.5.

## 5 Creation of Morphing Dataset

We train a network as described in Section 3. We create two sets of morphs using the validation set, the first using the landmark-based method and the second using the embedding-based approach.

Table 1: Training and validation sets.

	Training	Validation
# real IDs	482	86
# real imgs	18,143	3,629
# morph IDs	-	115
# morph imgs (embedding)	-	7,410
# morph imgs (landmark)	-	22,230

We use a dataset of in total 21,772 facial images, which is the subset of all portrait images provided in the FRGC dataset [25]. For each identity in the validation set, we select the next four most similar identities. We do this because selecting

identities that resemble each other leads to more challenging morphs than e.g. randomly selecting pairs of identities for morphing [26].

We define a mean embedding for each identity by computing the embedding returned by Dlib for each image of that identity and averaging these embeddings, i.e. the mean embedding for the  $i$ -th identity is

$$\bar{z}_i = \frac{1}{N_i} \sum_{k_i=1}^{N_i} f(I_{k_i}), \quad (5)$$

where the  $I_{k_i}$  is an image of the  $i$ -th identity,  $N_i$  is the number of available images of the  $i$ -th identity and  $f$  is defined as in Section 3.1. For each identity  $i$  we select four most similar identities by finding those  $z_j, j \neq i$  that have the smallest euclidean distance to  $z_i$ . This results in  $4 \cdot 482 = 1928$  pairs of identities. We remove any duplicate pairs and split the dataset of normal images into training and validation set, see Table 1. We generate morphed images using only those identity pairs for which both identities are in the validation set to prevent any overlap between training and validation set, after which 115 pairs of identities remain. For each identity pair ( $id_1, id_2$ ) we then randomly select image pairs from the subset of faces with neutral expression and create landmark-based morphs as described in Fig. 1. Both warping and blending parameter are set to 0.5. We generate embedding-based morphs by passing embeddings through the Decoder as described in Section 3.1. For each pair of images ( $Im_1, Im_2$ ) selected for morphing we create one embedding-based morph and three landmark-based morphs: one full morph (with ghosting artifacts in the background) and two spliced morphs, resulting in 7,410 embedding-based morphs and 22,230 landmark-based morphs. An example is shown in Fig. 3.

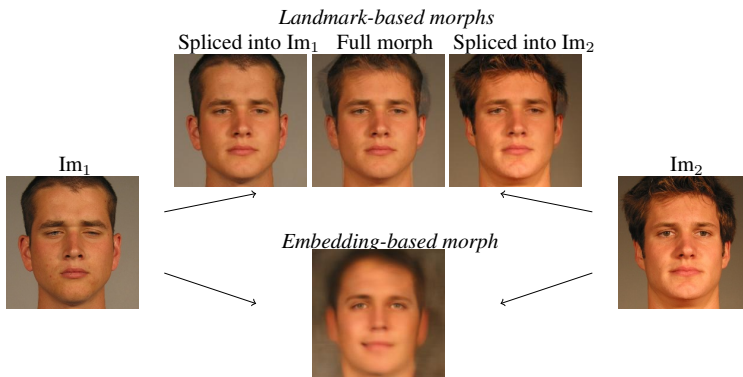


Figure 3: Embedding-based and landmark-based morphs.

## 6 Results & Discussion

We first examine the resulting embedding-based morphs using the same FRS (Dlib) used to generate them. The resulting histograms of genuine, impostor and morph scores are shown in Fig. 4. The left half of what seems like a bi-modal distribution of the morph scores seems to be caused by the fact that there are certain impostor pairs (the impostor pairs that lead to scores between approximately 0.4 and 0.6.) that contribute to a higher false match rate. These include several non-white faces that are considered similar by the FRS. The MMPMR for the embedding-based morphs is 65.2%, while it is close to 100% for landmark-based morphs. This means that the majority of the embedding-based morphs contain enough identity information of the two contributing identities to fool the FRS, if not as consistently as the landmark-based morphs.

Since the decoder network is trained using a pixel-based loss, this leads to the output images being blurry, especially outside the facial area. The fact that the images do not convincingly look like real images may cause the lower MMPMR for embedding-based morphs. This might be resolved by improving the realism of the output images, which could for example be achieved by only training the decoder to reconstruct a region of interest and splicing the morph into a different background, just as is done for landmark-based morphs. Another option to improve reconstruction quality would be to introduce a discriminating loss, as is done in GANs. In that case, the approach becomes more similar to existing GAN-based morphing techniques, with the difference that embedding-based morphs depend on worst-case embeddings.

Another improvement may be realised by adapting the pixel-based loss, since it is not ideal for preserving identity information. If the FRS's mapping  $f$  to embedding space is known and we can backpropagate gradients through it, we

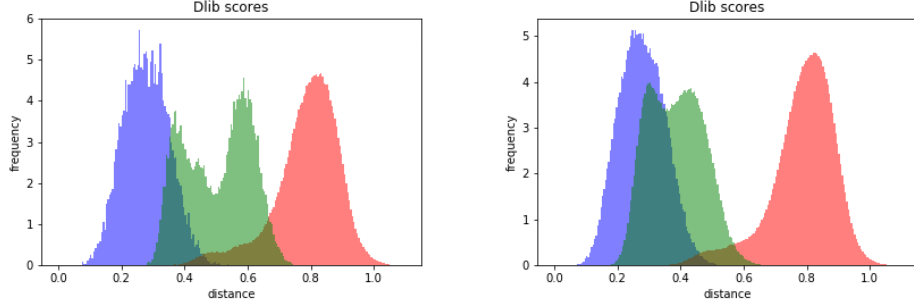


Figure 4: Vulnerability of dlib face recognition to embedding-based morphs (top) and landmark-based morphs (bottom). The blue histograms describe the genuine comparison scores, red the impostor comparison scores and green the morph scores (morph compared to a different image of one of the contributors).

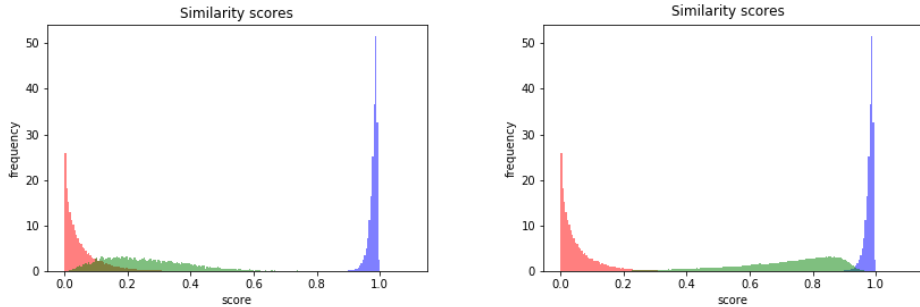


Figure 5: Vulnerability of FaceVacs face recognition to embedding-based morphs (top) and landmark-based morphs (bottom). Blue: genuine scores, red: impostor scores, green: morph scores. While few morph comparison scores are above the decision threshold of 0.5, they are significantly larger than the impostor comparison scores.

can extend the loss function in Eq. 4 with a term that encourages the network to return an image that maps onto the embedding it was given as input

$$\mathcal{L}_{\text{rec}}^i = \|z^i - f(f^{-1}(z^i))\|_2. \quad (6)$$

The loss function can then be extended to

$$\mathcal{L} = \frac{1}{M} \sum_{i=1}^M \mathcal{L}^i + \alpha \mathcal{L}_{\text{rec}}^i,$$

where  $\alpha > 0$  is the weight given to reconstructing the input embedding. In this case the attacks may become more similar to adversarial attacks and do not necessarily result in visually convincing images. This may be prevented by using for example a combination of different FRSs to estimate the reconstruction loss in Eq. 6. If the mapping of an FRS is unknown, but the embeddings corresponding to a set of images are given, we can train an approximation of the original FRS and use this to calculate the loss given in Eq. 6.

The embedding-based morphs are also not as challenging for the Cognitec FRS (MMPMR $\approx$ 0.9%) as landmark-based morphs (MMPMR $\approx$ 90%), see Fig. 5. This is not entirely surprising, since our method is trained to generate approximations of worst-case morphs specifically for one FRS, which does not necessarily generalise to other FRSs. The morph comparison scores are however significantly different from the impostor scores, indicating that they may still pose a risk. Especially if the morphs are further improved, they may be useful in understanding an FRS’s vulnerability.

## 7 Conclusion & Future Work

We introduced the concept of worst-case morphs, which are morphs that are most similar to the contributing identities according to an FRS. We trained a decoder network to generate embedding-based morphs that approximate such worst-case morphs. The majority of these morphs successfully fooled the FRS they were trained to fool. However, they were not (yet) as successful as landmark-based morphs. We also showed that this does not necessarily translate to the ability to fool other FRSs. We suggested several possible ways to improve the approximation of worst-case morphs.

Embedding-based approximations of worst-case morphs do not yet fool FRSS to the same extent that landmark-based morphs do. However, they can be helpful in understanding and visualising the vulnerabilities of FRSS, and may also offer some insight into the robustness of MAD techniques. Furthermore, our approach has the advantage of being far more robust to train than GANs.

Since GAN-based methods are currently the only existing alternative for generating morphs that are different from landmark-based morphs, our method is a valuable contribution to creating more varied morph databases.

For now though, Face Recognition Systems can rest easy knowing that embedding-based morphs are more a bad dream than a nightmare.

## References

- [1] M. Ferrara, A. Franco, and D. Maltoni. The magic passport. In *IEEE International Joint Conference on Biometrics*, pages 1–7, 2014.
- [2] U. Scherhag, C. Rathgeb, J. Merkle, R. Breithaupt, and C. Busch. Face recognition systems under morphing attacks: A survey. *IEEE Access*, 7:23012–23026, 2019.
- [3] D. Robertson, R. Kramer, and A. Burton. Fraudulent ID using face morphs: Experiments on human and automatic recognition. *PLOS ONE*, 12:e0173319, 03 2017.
- [4] A. Makrushin and A. Wolf. An overview of recent advances in assessing and mitigating the face morphing attack. In *2018 26th European Signal Processing Conference (EUSIPCO)*, pages 1017–1021, 2018.
- [5] U. Scherhag, C. Rathgeb, and C. Busch. Performance variation of morphed face image detection algorithms across different datasets. In *2018 International Workshop on Biometrics and Forensics (IWBF)*, pages 1–6, 2018.
- [6] L. Spreeuwers, M. Schils, and R. Veldhuis. Towards robust evaluation of face morphing detection. In *2018 26th European Signal Processing Conference (EUSIPCO)*, pages 1027–1031, 2018.
- [7] Ministerie van Binnenlandse Zaken en Koninkrijksrelaties, <https://www.government.nl/topics/identification-documents/requirements-for-photos>, accessed: 08-06-2020.
- [8] Kiran Raja, Matteo Ferrara, Annalisa Franco, Luuk Spreeuwers, Ilias Batskos, Florens Frans de Wit, Marta Gomez-Barrero, Ulrich Scherhag, Daniel Fischer, Sushma Venkatesh, Jag Mohan Singh, Raghavendra Ramachandra, Christian Rathgeb, Dinusha Frings, Uwe Seidel, Fons Knopjes, Raymond N.J. Veldhuis, Davide Maltoni, and Christoph Busch. Morphing attack detection - database, evaluation platform and benchmarking. *IEEE transactions on information forensics and security*, 16:4336–4351, 2021.
- [9] NIST FRVT MORPH, [https://pages.nist.gov/frvt/html/frvt\\_morph.html](https://pages.nist.gov/frvt/html/frvt_morph.html), accessed: 05-10-2021.
- [10] Bologna Online Evaluation Platform (BOEP) - Morph Attack Detection Evaluation, <https://biolab.csr.unibo.it/fvcongoing/UI/Form/BOEP.aspx>, accessed: 05-10-2021.
- [11] Haoyu Zhang, Sushma Venkatesh, Raghavendra Ramachandra, Kiran Raja, Naser Damer, and Christoph Busch. Mipgan—generating strong and high quality morphing attacks using identity prior driven gan. *IEEE Transactions on Biometrics, Behavior, and Identity Science*, 3(3):365–383, 2021.
- [12] S. Venkatesh, H. Zhang, R. Ramachandra, K. Raja, N. Damer, and C. Busch. Can GAN generated morphs threaten face recognition systems equally as landmark based morphs? - vulnerability and detection. In *2020 8th International Workshop on Biometrics and Forensics (IWBF)*, pages 1–6, 2020.
- [13] C. Seibold, A. Hilsmann, and P. Eisert. Style your face morph and improve your face morphing attack detector. In *2019 International Conference of the Biometrics Special Interest Group (BIOSIG)*, pages 1–6, 2019.
- [14] M. Ferrara, A. Franco, and D. Maltoni. Face morphing detection in the presence of printing/scanning and heterogeneous image sources. *IET Biometrics*, 10(3):290–303, 2021.
- [15] S. Venkatesh, K. Raja, R. Ramachandra, and C. Busch. On the influence of ageing on face morph attacks: Vulnerability and detection. In *2020 IEEE International Joint Conference on Biometrics (IJCB)*, pages 1–10, 2020.
- [16] N. Damer, A. M. Saladié, A. Braun, and A. Kuijper. Morgan: Recognition vulnerability and attack detectability of face morphing attacks created by generative adversarial network. In *2018 IEEE 9th International Conference on Biometrics Theory, Applications and Systems (BTAS)*, pages 1–10, 2018.
- [17] Rameen Abdal, Yipeng Qin, and Peter Wonka. Image2stylegan: How to embed images into the StyleGAN latent space? In *2019 IEEE/CVF International Conference on Computer Vision (ICCV)*, pages 4431–4440, 2019.

- [18] A. Creswell, T. White, V. Dumoulin, K. Arulkumaran, B. Sengupta, and A. Bharath. Generative adversarial networks: An overview. *IEEE Signal Processing Magazine*, 35(1):53–65, 2018.
- [19] U. Scherhag, J. Kunze, C. Rathgeb, and C. Busch. Face morph detection for unknown morphing algorithms and image sources: a multi-scale block local binary pattern fusion approach. *IET Biometrics*, 9(6):278–289, 2020.
- [20] K. He, X. Zhang, S. Ren, and J. Sun. Deep residual learning for image recognition. *CoRR*, abs/1512.03385, 2015.
- [21] Davis E. King. Dlib-ml: A machine learning toolkit. *Journal of Machine Learning Research*, 10:1755–1758, 2009.
- [22] Gary B. Huang, Manu Ramesh, Tamara Berg, and Erik Learned-Miller. Labeled faces in the wild: A database for studying face recognition in unconstrained environments. Technical Report 07-49, University of Massachusetts, Amherst, October 2007.
- [23] FaceVACS 9.4.0. <http://www.cognitec-systems.de> (2019).
- [24] U. Scherhag, A. Nautsch, C. Rathgeb, M. Gomez-Barrero, R. N. J. Veldhuis, L. Spreeuwens, M. Schils, D. Maltoni, P. Grother, S. Marcel, R. Breithaupt, R. Ramachandra, and C. Busch. Biometric systems under morphing attacks: Assessment of morphing techniques and vulnerability reporting. In *2017 International Conference of the Biometrics Special Interest Group (BIOSIG)*, pages 1–7, 2017.
- [25] P. J. Phillips, P. J. Flynn, T. Scruggs, K. W. Bowyer, Jin Chang, K. Hoffman, J. Marques, Jaesik Min, and W. Worek. Overview of the face recognition grand challenge. In *2005 IEEE Computer Society Conference on Computer Vision and Pattern Recognition (CVPR'05)*, volume 1, pages 947–954 vol. 1, 2005.
- [26] Naser Damer, Alexandra Moseguí Saladié, Steffen Zienert, Yaza Wainakh, Philipp Terhörst, Florian Kirchbuchner, and Arjan Kuijper. To detect or not to detect: The right faces to morph. In *2019 International Conference on Biometrics (ICB)*, pages 1–8, 2019.